

ADDIS ABABA UNIVERSITY  
SCHOOL OF POST GRADUATE STUDIES



**COMPARATIVE STUDY ON SOLID-STATE PHOTOELECTROCHEMICAL  
SOLAR ENERGY CONVERSION BASED ON P3OT AND P3OT: PCBM**

***By : Kassa Derib***

**Advisor : Prof. Teketel Yohannes**

---

A Project Report Submitted To The School Of Graduate Studies In Partial  
Fulfillment Of The Requirements For The Degree Of Master Of Science In  
Chemistry

---

June, 2010

## **ACKNOWLEDGEMENTS**

I am deeply indebted to Prof. Teketel Yohannes for his invaluable guidance, genuine concern to help in any aspect, unreserved support, constant encouragement and comments on the work through out the study.

I would like to express gratitude gratefulness to Ato Sisay Tadesse for his concern he has shown, and the suggestions and encouragement he has offered to me during the course of this work. Ato Getachew Adam have also unforgettable contribution to my work.

I am very much thankful to Dr Mesifn Redi and Dr Ahmed Mustefa for there encouragement and also thank my friend Daniel Manaye and Anteneh Wodage.

I do not have any words to thank my wife Nestanet Wagaw, who stayed with me in times of failure, success, happiness and hardships.

Last but not least, I would like to acknowledge my father, mother, brother and sisters.

# TABLE OF CONTENTS

CONTENT	Page
<b>Acknowledgements</b> .....	i
<b>Table of content</b> .....	ii
<b>List of Figures</b> .....	iv
<b>Abstract</b> .....	vi
1. INTRODUCTION.....	1
2. LITERATURE REVIEW .....	3
2.1. Electronically Conducting Polymers.....	3
2.2. Charge Transport Mechanism .....	4
2.3. Ionically Conducting Polymers .....	5
2.4. Conducting Polymer-PCBM Heterojunction Solar Cells.....	6
2.5. Photoelectrochemical Solar Energy Conversion.....	8
2.5.1. Introduction.....	8
2.5.2. Semiconductor/Electrolyte Interface.....	8
2.5.3. Photoinduced Charge Transfer Reaction at the Interface.....	10
2.6. Solar Cell Parameters .....	11
3. OBJECTIVE .....	15
4. EXPERIMENTAL.....	15
4.1. Materials and Chemicals.....	15
4.2. Experimental Set-up.....	16
4.3. Procedure.....	17
4.3.1. ITO-Coated Glass Preparation.....	17

4.3.2. Solution preparation.....	17
4.3.3. Quasi Reference Electrode Preparation.....	17
4.3.4. Electropolymerization.....	17
4.3.5. Preparation of The polymer P3OT and P3OT:PCBM films on ITO.....	18
4.3.6. Devices Structures .....	18
5. RESULTS AND DISCUSSION.....	19
5.1. Current-voltage Characteristics.....	19
5.2. Transient Studies .....	22
5.3. Spectral Response.....	25
5.4. $I_{sc}$ dependence on incident light intensity .....	26
5.5. $V_{oc}$ dependence on incident light intensity .....	28
6. CONCLUSIONS.....	30
7. REFERENCES.....	31

## LIST OF FIGURES

Figure	Page
2.1. Chemical structures of some conjugated polymers.....	4
2.2. Intersoliton hopping in <i>trans</i> -polyacetylene.....	5
2.3. Photoelectrochemical cell.....	8
2.4. Representation of the formation of the Schottky junction between a p-type semiconductor and an electrolyte containing a redox couple O/R.....	10
2.5. Typical current density-voltage characteristics of Schottky diodes.....	12
4.1. Chemical structure of (a) P3OT, (b) PEDOT and (c) PCBM.....	15
4.2. General experimental set-up for the photoelectrochemical measurements.....	16
4.3. The basic structure of the solid-state PECs.....	18
5.1. Current-voltage characteristics of ITO   P3OT   POMOE:I <sub>3</sub> <sup>-</sup> /I <sup>-</sup>   PEDOT   ITO in the dark and light from the front side illumination with light intensity of 100 mWcm <sup>-2</sup> .....	19
5.2. Current-voltage characteristics of ITO   P3OT:PCBM   POMOE:I <sub>3</sub> <sup>-</sup> /I <sup>-</sup>   PEDOT   ITO PECs in the dark and under illumination through front side with light intensity of 100 mWcm <sup>-2</sup> .....	20
5.3. Photocurrent response to switching illumination on and off from the front side of the P3OT based solid-state PEC with a light intensity of 100 mW/cm <sup>2</sup> .....	22
5.4. Photocurrent response to switching illumination on and off from the front side of the P3OT:PCBM based solid-state PEC with a light intensity of 100 mW/cm <sup>2</sup> .....	23
5.5. Photovoltage response to switching illumination on and off from the front side of the P3OT based solid-state PEC with a light intensity of 100 mW/cm <sup>2</sup> .....	24
5.6. Photovoltage response to switching illumination on and off from the front side of the P3OT:PCBM based solid-state PEC with a light intensity of 100 mW/cm <sup>2</sup> .....	24
5.7. Photocurrent action spectra through (a) front side and (b) back side of ITO   P3OT:PCBM   POMOE:I <sub>3</sub> <sup>-</sup> /I <sup>-</sup>   PEDOT   ITO PEC with monochromatic light.....	25
5.8. Dependence of I <sub>sc</sub> on incident light intensity of P3OT from front side	

illumination.....	27
5.9. Dependence of $I_{sc}$ on incident light intensity of P3OT:PCBM from the front side	
illumination.....	27
5.10. Dependence of $V_{oc}$ on incident light intensity of P3OT from front side	
illumination.....	28
5.11. Dependence of $V_{oc}$ on incident light intensity of P3OT:PCBM from front side	
illumination .....	29

## LIST OF TABLES

Table	Page
1. The HOMO and LUMO energy levels and band gap of P3OT, PCBM and C <sub>60</sub> .....	7
2. The photoelectrochemical parameters obtained from I-V measurements under the same illumination condition for pure P3OT and P3OT:PCBMphotoactive electrode based solid state PECs.....	21

## ABSTRACT

The photoelectrochemical properties of a solid-state photoelectrochemical cell (PEC) based on poly(3-octylthiophene), P3OT, and a blend of P3OT with phenyl-C<sub>61</sub>-butyric acid methyl ester, PCBM, an ion-conducting polymer electrolyte, amorphous poly(ethylene oxide), POMOE, complexed with iodine/triiodide redox couple has been constructed and studied. The current - voltage characteristics in the dark and under white light illumination, the dependence of the short - circuit ( $I_{sc}$ ) and the open - circuit voltage ( $V_{oc}$ ) of the two types of the devices have been compared. An open-circuit voltage of 344 mV and a short-circuit current of  $0.47 \mu\text{A cm}^{-2}$  were obtained for the device of P3OT as a photoactive electrode and an open-circuit voltage of 294 mV and a short-circuit current of  $4.271 \mu\text{A cm}^{-2}$  were obtained for the device of P3OT:PCBM at light intensity of  $100 \text{ mW/cm}^2$ . The transient photocurrent and photovoltage, the photocurrent action spectra of the blend P3OT:PCBM for front and back side illuminations and an open-circuit voltage and short-circuit current dependence on light intensity have been studied. During illumination, a cathodic photocurrent was observed, indicating that the neutral poly(3-octylthiophene) behaves as a p-type semiconductor. IPCE% of 0.0682 % for front side illumination (ITO/PEDOT) and IPCE% of 0.0011 % for backside illumination (ITO/P3OT:PCBM) were obtained for the device ITO | P3OT:PCBM | POMOE:I<sub>3</sub><sup>-</sup>/I<sup>+</sup> | PEDOT | ITO.

## **INTRODUCTION**

It is expected that the global energy demand will double within the next 50 years. Fossil fuels, however, are running out and are held responsible for the increased concentration of carbon dioxide in the earth's atmosphere. Hence, developing environmentally friendly, renewable energy is one of the challenges to society in the 21<sup>st</sup> century. One of the renewable energy technologies is photovoltaics (PV), the technology that directly converts daylight into electricity. PV is one of the fastest growing of all the renewable energy technologies; in fact, it is one of the fastest growing industries at present. Solar cell manufacturing based on the technology of crystalline, silicon devices is growing by approximately 40 % per year and this growth rate is increasing [1].

The current status of PV is that it hardly contributes to the energy market, because it is far too expensive. The large production cost for the silicon solar cells is one of the major obstacles. Even when the production costs could be reduced, large-scale production of the current silicon solar cells would be limited by the scarcity of some elements required, e.g. solar-grade silicon. To ensure a sustainable technology path for PV, efforts to reduce the costs of the current silicon technology need to be balanced with measures to create and sustain variety in PV technology. It is, therefore, clear that 'technodiversity', implying new solar cell technologies, is necessary [2].

Another approach is based on solar cells made of entirely new materials, conjugated polymers and molecules. Conjugated materials are organics consisting of alternating single and double bonds. The field of electronics based on conjugated materials started in 1977 when Heeger, MacDiarmid and Shirakawa discovered that the conductivity of the conjugated polymer polyacetylene can be increased by seven orders of magnitude upon oxidation with iodine [3, 4].

This has paved the way for the new class of semiconductor materials, which are typically inexpensive and easy to process. The discoveries of conjugated polymers with semiconductor-like properties are not only able to function in a similar way to inorganic semiconductor but also have important advantages. These include their being low cost, light weight, easy to fabricate and potentially manufacturable as large-area coatings. The use of such polymers as photoactive electrodes is of increasing interest as the processing possibilities of these materials become more developed. Over and above this, the high

absorption coefficients of these materials and the possibility of varying the band gap through molecular engineering has paved the way for new options for solar-energy conversion [3].

Organic photovoltaic solar cells with blends of conjugated polymers and fullerenes have been extensively studied [5-7]. A less expensive solar energy conversion can be achieved by photoelectrochemical (PEC) cells, which involve the use of semiconductor to absorb incident light and an electrochemical process at semiconductor/liquid junction to allow energy conversion.

Organic PEC grasp increasing research attention recently is the solid-state PECs with the ion conducting solid polymer electrolyte. These cells compared to liquid electrolyte PECs possess advantages such as handling, portability and packing. Previous studies on the solid state PECs were focused on use of pure conjugated semiconducting polymer [8-11], copolymers [12] and a mixture of conjugated polymer with fullerene [13, 14] as a photoactive electrode.

Solid state photoelectrochemical solar cell based on conjugated polymer mixed with phenyl-C<sub>61</sub>-butyric acid methyl ester (PCBM), which is a fullerene derivative of the C<sub>60</sub> buckyball as a photoactive electrode has not yet studied. Though PCBM has similar function with C<sub>60</sub>, in PCBM, the fullerene cage carries a substituents that prevents extensive crystallization upon mixing with the conjugated polymer and enhances the miscibility [15]. The use of conjugated polymer/fullerene and fullerene derivatives blends as photoactive electrodes give ultrafast electron transfer from optically excited polymer to PCBM [16], resulting in improvements of photocurrent [13,14].

The aim of this work is thus, to construct and study solid state PECs consisting conjugated semiconducting polymer and a blends of conjugated semiconducting polymer with PCBM as photoactive electrode, and ion conducting solid polymer electrolyte complexed with a redox couple.

## **2. LITERATURE REVIEW**

### **2.1. Electronically Conducting Polymers**

Polymers are macromolecules consisting of a great number of repeating units, which are coupled to each other by covalent bonds to form a long chain. These repeating units can be any group of atoms, however, we consider only organic polymers, where the backbone consists of only carbon. Most organic polymers that have side chains are soluble in organic solvents. The solvents easily evaporate upon spin coating or solvent casting, leaving thin films on a substrate [17].

Conjugated polymers have recently attracted a great amount of interest as conducting and semiconducting materials. Because organic materials can be processed at low temperature, they can be fabricated into thin films onto plastic substrates. The extensive delocalization of  $\pi$ -electrons is well known to be responsible for the array of remarkable characteristics that these polymers tend to exhibit. These properties include non-linear optical behavior, electronic conductivity and exceptional mechanical properties such as tensile strength and resistance to harsh environments [18]. A conducting polymer possesses the electrical, electronic, magnetic, and optical properties of a metal while retaining the mechanical properties, processibility, etc. commonly associated with a conventional polymer. Polymers composed of aromatic and heteroaromatic ring structures have been particularly outstanding from materials perspective [19]. There exist different kinds of conjugated polymers out of which some are depicted in Fig. 2.1.

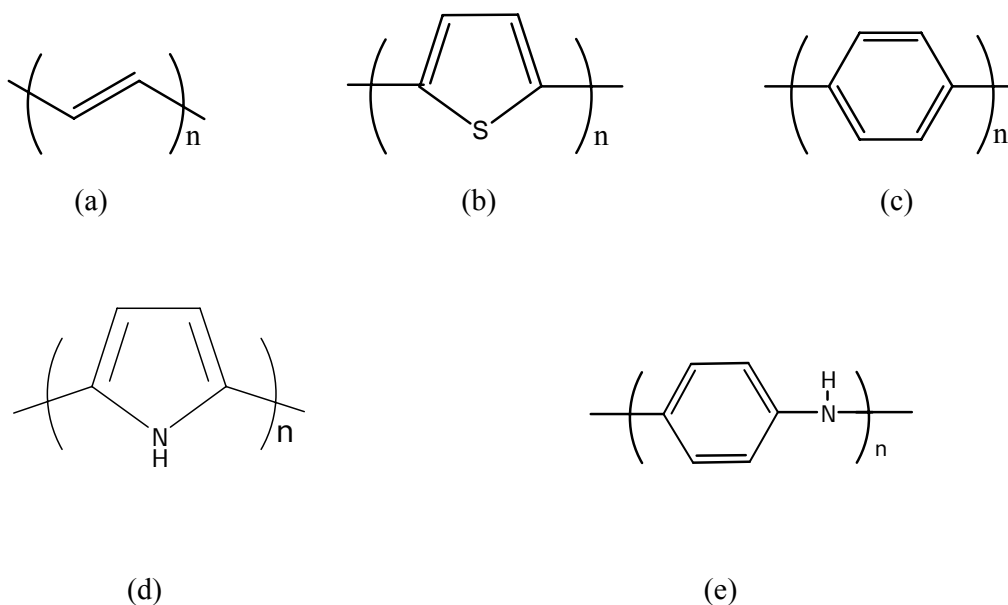


Fig. 2.1. Chemical structures of some conjugated polymers, (a) *trans*-polyacetylene, (b) polythiophene, (c) poly(*p*-phenylene), (d) polypyrrole and (e) polyaniline

## 2.2. Charge Transport Mechanism

The prerequisite for charge transport is the presence of mobile charge carriers. In conducting polymers the conductivity is the presence of solitons, polarons and bipolarons, which are formed by self-localization of the carriers, induced into the  $\pi$  electronic systems through doping and in some cases during synthesis [20].

Conductivity of materials depends on temperature. The temperature dependence of polymer conductivity is manifested opposite to that of metals. In case of conjugated polymers conductivity depends on doping level. At low doping levels the temperature dependence of the conductivity is high. As the doping level increases, the dependence of the conductivity on temperature becomes less [21].

There is no definite mechanism of charge transport and hence different models are suggested over the whole conductivity range. In the undoped form of conjugated polymers, the charge transport is similar to that of amorphous semiconductors. It is explained by hopping between localized states. At very low doping levels, the conductivity is mainly

due to hopping (phonon assisted quantum mechanical tunnelling). Its concept is generally deduced from ionic conduction to electronic conduction in amorphous and disordered non-metallic solids and polymers. In such materials we do not have free charge carriers, rather than localized electrons and so they can move between these localized states, which are distributed randomly.

For polyacetylene, where solitons are dominant charge carriers, intersoliton hopping is the dominant conductivity mechanism.

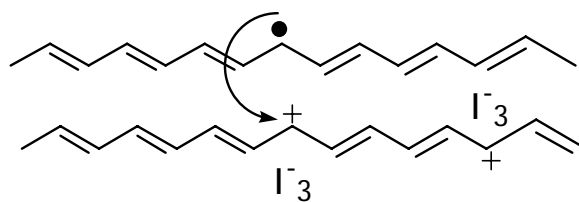


Fig. 2.2. Intersoliton hopping in *trans*-polyacetylene.

The charged solitons are trapped by the dopant ions and neutral solitons are free to move. When neutral soliton passes close by a charged soliton, an electron can hop between the mid gap states belonging to the solitons [22].

### 2.3. Ionically Conducting Polymers

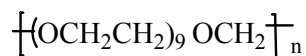
Electronic conductivity is the phenomenon related to the electrons-holes movement into solid conductors but ionic conductivity is described as the charge movement due to ions' motion. Electrolytes are materials that have high ionic but negligible electronic conductivity. Most electrolytes are liquids, either a molten salt or a salt dissolved in a liquid solvent [23].

The interest in these solid-state ionic conductors comes from the possibility of using them to substitute the liquid electrolytes in several electrochemical devices. The major challenge into replacing the liquid or gel electrolyte by a polymeric one is to keep the high operation efficiency, similar to the electrochemical devices based on liquid junctions. Besides improving the stability of the active interface, allowing a long-term durability, a polymer electrolyte eliminates problems concerning evaporation or leakage of the solvent.

Polymer electrolytes are complexes of metal salts with high molecular weight polymers containing electron donor atoms or groups of atoms that co-ordinate with the metal ion in the salt. To be successful as a host, a polymer should possess (a) electron donor atoms or groups of atoms (such as -O- ether, -S- sulphide, -N- amine, -P- phosphine, C=O carbonyl, and C≡N cyano) that form co-ordinate bonds with the cations, (b) low barriers to bond rotation for atoms in the main chain so that high flexibility and hence the segmental motion of the polymer chain can take place readily, and (c) a suitable distance between co-ordinating centres which ensures adequate jumping distance for charge carriers [23].

Poly(ethylene oxide), PEO, is the reference polymer for ionic conduction, since it is the best matrix for alkali salts because of the high Lewis base character of the oxygen atoms present in this polyether. PEO is a linear polymer and the regioregularity of the – (CH<sub>2</sub>-CH<sub>2</sub>O) – unit allows a high degree of crystallinity (70-85 %). The melting point of the crystalline phase is 65°C and the glass transition temperature (T<sub>g</sub>) is low, approximately -60°C, which do not permit ion transport at ambient temperatures. The dielectric constant is low (~5-8). One of the most successful amorphous host polymers is an oxyethylene-oxymethylene structure in which medium length but randomly variable ethylene oxide units are interspersed with methylene oxide groups [24].

The methylene oxide groups break up the regular helical structure of polyethylene oxide, thus suppressing crystallization. The amorphous polymer has the following general structural formula.



The redox couple used to complex with the polymer electrolyte is iodine/triiodide [25].

#### **2.4. Conducting Polymer-PCBM Heterojunction Solar Cells**

The highest efficiencies achieved so far are ~ 7.4 % under AM1.5 simulated solar spectrum for devices made from blends of conducting polymer and phenyl-C<sub>61</sub>-butyric acid methyl ester (PCBM) [26]. Significant efforts are being made to increase efficiencies through low band gap polymers, new acceptor materials, and novel processing approaches, and

improvement practical consideration such as stability and fabrication of large area devices are gaining more attention. Polymeric photovoltaic devices rely upon the dissociation of photogenerated exciton by the transfer of an electron from conjugated polymer donor to the acceptor species, because the exciton diffusion distance is limited to  $< 10$  nm [27].

PCBM is generally a preferred acceptor materials to  $C_{60}$  for organic photovoltaic devices and this is also true for PEC cell because the presence of the side chain enhances the solubility and the higher lowest unoccupied molecular orbitals (LUMO) energy level relative to  $C_{60}$  leads to a higher open circuit voltage,  $V_{oc}$  [28].

If the acceptor LUMO is sufficiently lower than the donor LUMO, the excited electrons will relax into the acceptor LUMO and in this separate from the holes. The photoinduced electron transfer with a sub picosecond transfer rate in blends of conducting polymer and  $C_{60}$  has provided a high efficiency photovoltaic conversion. Since the charge transfer takes place  $\sim 1000$  times faster than any decay of the photoexcitation [29].

There are two general ways to create a donor-acceptor interface in organic devices. One is to bring two films in contact at the surface, which creates a heterojunction. In this case, only a fraction of the bulk of the material builds a donor-acceptor interface. The other is to blend the two materials to form one mixed layer. In this case, the whole bulk of the device has a donor-acceptor interface. These devices are called bulk-heterojunction devices. The conducting polymer- fullerene bulk heterojunction solar cells leads to an enhancement of current density due to an increased interface area for charge separation. The HOMO and LUMO energy levels and energy gap of P3OT [6], PCBM [30] and  $C_{60}$  [31] are shown in table 1.

Table 1. The HOMO and LUMO energy levels and  $E_g$  of P3OT, PCBM and  $C_{60}$ .

Material	HOMO level (eV)	LUMO level (eV)	Band gap (eV)
P3OT	-5.25	-2.85	2.40
PCBM	-6.00	-3.90	2.10
$C_{60}$	-6.10	-3.70	2.40

## 2.5. Photoelectrochemical Solar Energy Conversion

### 2.5.1. Introduction

Photoelectrochemical solar energy conversion is based on the junction between a semiconductor and an electrolyte. A typical photoelectrochemical cell (PEC) is shown in Fig. 2.3. It consists of a semiconductor electrode, a counter electrode and an electrolyte containing a redox couple. The PECs that convert light into electricity are termed "electrochemical photovoltaic" or "regenerative cells" and those that generate chemical fuels are "photoelectrosynthetic" or "non-regenerative cells" [23].

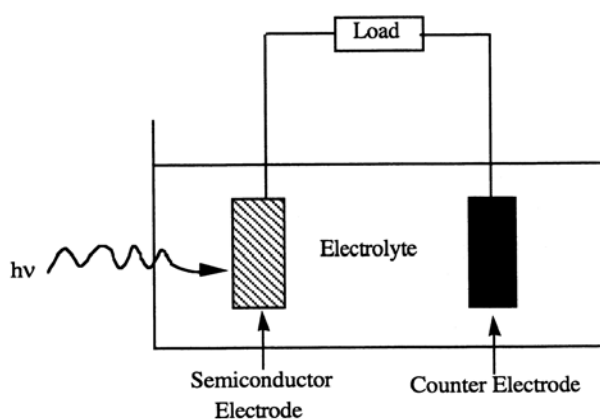


Fig. 2.3. Photoelectrochemical cell.

Semiconductors with large  $E_g$  are stable under illumination. However, they are inefficient for solar conversion, since they absorb only in the UV, where there is little solar radiation reaching the surface of our planet. The semiconductors that efficiently convert solar energy are those with small  $E_g$  because they capture a large fraction of the incident energy. However, they exhibit decomposition or passivation processes which compete with the desired energy conversion. This is a serious problem for liquid junction PECs [32].

### 2. 5. 2. Semiconductor/Electrolyte Interface

The PEC systems are based on the formation a semiconductor/electrolyte junction where an appropriate semiconductor is immersed in an appropriate electrolyte. The junction is characterized by the presence of a space charge layer in the semiconductor adjacent to the interface with the electrolyte. A space charge layer generally develops in a semiconductor

upon contact and equilibration with a second phase whenever the initial chemical potential of electrons is different for the two phases. The chemical potential of electrons is referred as redox potential for electrolyte and Fermi level for semiconductors. The Fermi level of a p-type material is just above their valance bands (VBs) and of an n-type material is below their conduction bands (CBs). The higher the concentration of the dopants the closer the Fermi level to the bands.

If the initial Fermi level in an n-type semiconductor is above the initial redox potential level in an electrolyte, then the equilibration of the chemical potentials occurs by the transfer of electrons from the semiconductor to the electrolyte. This produces a positive space charge layer in the semiconductor (also called depletion layer since the region is depleted of majority carriers). As result, the CB and VB edges are bent such that a potential barrier is established against further electron transfer into the electrolyte. The barrier height, the difference between the Fermi level of the semiconductor ( $E_f$ ) and the potential of the redox couple ( $E_{\text{redox}}$ ), represents the upper limit of the open circuit voltage,  $V_{\text{oc}}$ , which can be achieved under high irradiance.  $V_{\text{oc}}$  cannot exceed ( $E_f - \text{VB}$ ) for photoanodes and ( $E_f - \text{CB}$ ) for photocathodes [33, 34].

The inverse but analogous situation occurs with p-type semiconductors having an initial Fermi level below that of the electrolyte. A negative space charge is formed in semiconductor, with the VB and CB being produce a potential barrier against further positive hole transfer into the electrolyte. A charged layer, called Helmholtz layer, also exists in the electrolyte adjacent to the interface with the solid electrode. This layer consists of a charge ions from the electrolyte adsorbed on the solid electrode surface. The potential drop across the Helmholtz layer depends upon the specific ionic equilibrium at the interface. A very important consequence of the Helmholtz layer of semiconductor electrodes is that it markedly affects the band bending.

Because of the high charge density and small width of the Helmholtz layer, the potential difference across it does not vary with applied potential or charge transfer across the semiconductor/electrolyte interface. Instead, all of any external applied voltage appears across the depletion layer in the semiconductor. Consequently, at a given electrolyte composition the band edges of the semiconductor at the surface are fixed with respect to

the redox potential of the electrolyte, and independent of an applied voltage across the semiconductor electrolyte interface [35].

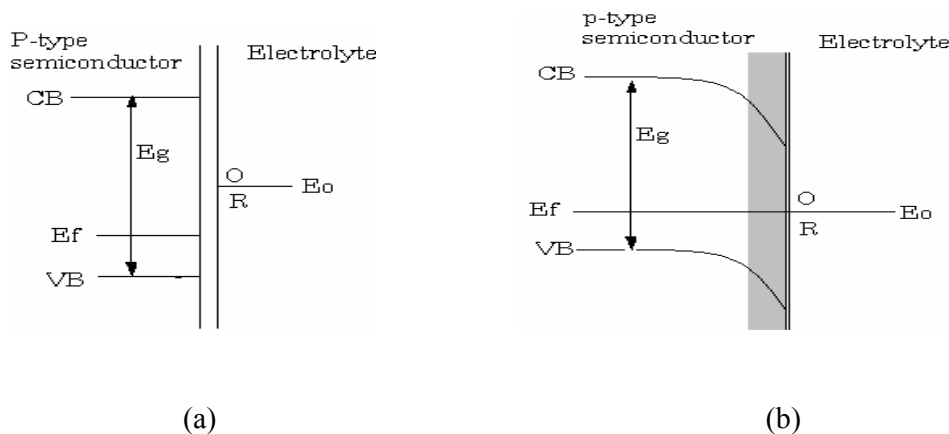


Fig. 2.4. Representation of the formation of the Schottky junction between a p-type semiconductor and an electrolyte containing a redox couple O/R: (a) before the contact, (b) after the contact, considering the redox potential of the electrolyte is higher than the semiconductor Fermi level.

### 2.5.3. Photoinduced Charge Transfer Reaction at the Interface

To convert solar energy into electrical and/or chemical energy, current must flow across the semiconductor/electrolyte junction. When an n-type semiconductor/electrolyte junction is illuminated with light, photons having energies greater than the semiconductor band gap are absorbed. In the dark, no current flows in the cell. But when it is illuminated, electrons are freed in the valence band and move into the conduction band. The free charges can then be separated under the influence of the electric field present in the space charge region. The electric field at the space charge does not require a constant energy input from an external source; rather, it occurs spontaneously whenever two phases with different electrochemical potentials are brought into contact. Electron - hole pairs produced by absorption of photons beyond the depletion layer will separate if the minority carriers can diffuse to the depletion layer before recombining with majority carriers. If they do not disappear by recombination, either by direct coulombic interaction or by collision with other carriers in their path through the space charge layer, the minority carriers in the semiconductor are swept to the surface where they are subsequently injected into the electrolyte to drive a redox reaction. On the other hand, the majority carriers are swept towards the semiconductor bulk, where

they subsequently leave the semiconductor *via* an ohmic contact and are then ejected at the counter electrode to drive a redox reaction opposite to that occurring at the semiconductor electrode. Since the electrons and holes travel in opposite directions, a continuous current will flow as long as the cell is illuminated and connected to an external load. The type of the redox species used is governed by the type of the semiconductor and the position of the energy bands. For *n*-type semiconductors, minority holes are injected to produce an oxidation reaction, while for *p*-type semiconductors, minority electrons are injected to produce a reduction reaction. Oxidations for *n*-type semiconductors will occur from holes in the valence band if the solution species Fermi level lies above the surface valence band level and reductions for *p*-type semiconductors will occur from electrons in the conduction band if the solution species Fermi level lies below the surface conduction band level.

The photogeneration causes the Fermi level in the semiconductor to return towards its original position, before the semiconductor/electrolyte junction was established. Under open circuit conditions between an illuminated semiconductor electrode and a metal counter electrode, a photovoltage is produced. The photovoltage produced between the electrodes is equal to the difference between the Fermi level in the semiconductor and the redox potential of the electrolyte. Under closed circuit conditions, the Fermi level in the system is equalized and no photovoltages exist between the two electrodes [23].

## 2.6. Solar Cell Parameters

The equations that describe the solar cell output parameters are given below [32, 36]. To derive this solar cell output parameters that are used for characterization of PEC properties of the device; we shall consider an ideal Schottky diode. When the cell is illuminated, the total current density,  $I$ , is equal to the sum of the photocurrent density,  $I_{ph}$ , and the dark current density,  $I_{dark}$ .

$$I = I_{ph} - I_{dark} \quad (1)$$

The dark current-voltage characteristics of the solar cell is expressed as

$$I = I_0 \left[ \exp\left(\frac{qV}{nkT}\right) - 1 \right] \quad (2)$$

The I-V characteristic of an illuminated semiconductor is given by:

$$I = I_{ph} - I_0 \left[ \exp\left(\frac{qV}{nkT}\right) - 1 \right] \quad (3)$$

Where  $I$  is the total current density (dark current density),  $I_0$  is the inverse saturation current density which is the current density flowing under sufficiently high reverse bias,  $q$  is the charge on an electron,  $V$  is the applied voltage,  $n$  is the ideality factor of the diode (for an ideal diode  $n = 1$ ),  $k$  is the Boltzmann constant and  $T$  is the absolute temperature.

The ideal I-V characteristic of the solar cell under illumination is shown in the following Fig. 2.5.

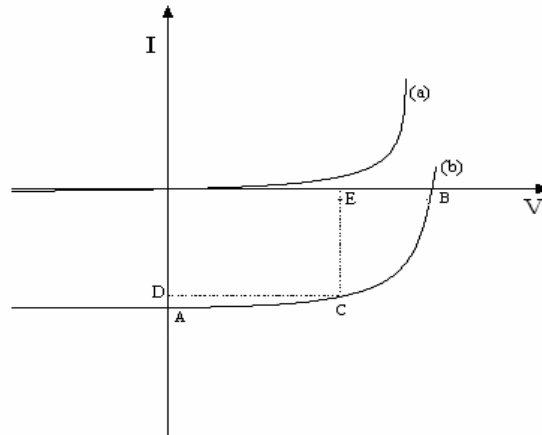


Fig. 2.5. Typical current density-voltage characteristics of Schottky diodes (a) in the dark (b) under illumination.

**(a) Short-circuit current ( $I_{sc}$ )**

The maximum current that can run through the cell is determined by the short-circuit current. It provides the measure of the collection efficiency of photon generated carriers in a particular PEC. This is extracted at zero applied voltage. It is obtained by substituting  $V = 0$  into Eqn. (3). Ideally it is equal to the current density,  $I_{ph}$ , generated by light.

$$I_{sc} = I_{ph} \quad (4)$$

**(b) Open-circuit voltage ( $V_{oc}$ )**

It is the maximum voltage attainable in a solar energy conversion device that can be extracted from an illuminated semiconductor/electrolyte interface. The open-circuit voltage of a solar cell under light is defined as a voltage at which the net current in the cell is equal to zero. This is the condition where photovoltage is generated but no photocurrent flows (point B in Fig. 2.5).  $V_{oc}$  is determined from the I-V curve as the point at which the curve crosses the voltage axis ( $I = 0$ ).  $V_{oc}$  can be calculated as follows

$$V_{oc} = \frac{nkT}{q} \ln \left( \frac{I_{ph}}{I_0} + 1 \right) \quad (5)$$

**(c) Fill factor (FF)**

Is the measure of the power that can be extracted from the cell and is defined as

$$FF = \frac{V_{mp} I_{mp}}{V_{oc} I_{sc}} \quad (6)$$

Where  $V_{mp}$  and  $I_{mp}$  are the voltage and the current at the maximum power point, respectively. The shape of the I-V curve is a measure of the FF. Rectangular shapes gives higher FF values.

**(d) Power conversion efficiency ( $\eta$ )**

The energy conversion efficiency of the solar cell in converting light energy into useful electrical energy is the most important quantity defining the quality of the cell. It is defined as the maximum power produced by the cell ( $P_{MAX}$ ) divided by the power of the incident light on the representative area of the cell ( $P_{in}$ ) and is given by

$$\eta = \frac{V_{mp} I_{mp}}{P_{in}} = \frac{V_{oc} I_{sc} FF}{P_{in}} \quad (7)$$

**(e) Incident monochromatic photon to current conversion efficiency (IPCE)**

One of the most important parameters when studying the performance of solar cells is the incident photon to current conversion efficiency, IPCE. It is defined as the ratio of the number of collected charge carriers to the number of incident photons at the device. As the name suggests, the value is commonly measured for a specific light wavelength. One advantage of analyzing the IPCE rather than photocurrent is that effects due to the spectral shape of the incident light, due to light source or measurement equipment, are removed and the true response of the device is obtained. Understanding the reasons for obtaining a specific IPCE of a device is essential to obtain fundamental understanding and thus to improve the device performance. Plots of IPCE versus wavelength illustrate the spectral operation range of a specific solar cell. For high performance solar cells, the IPCE value can reach unity over a large spectral section. The IPCE were calculated as the ratio of the observed photocurrent density and the photon density incident on the cell:

$$IPCE\% = \frac{1240I_{sc}}{\lambda P_{in}} \quad (8)$$

where  $I_{sc}$  is short circuit current ( $\mu\text{A cm}^{-2}$ ),  $\lambda$  the excitation wavelength (nm) and  $P_{in}$  the incident photon intensity ( $\text{Wm}^{-2}$ ). Light of different wavelength is absorbed at different depths of the photoactive electrode.

### **3. OBJECTIVE**

The objective of this project is to construct and study solid state PEC based on blend P3OT and PCBM photoactive material and compare the result to PEC constructed using P3OT photoactive electrode.

## 4. EXPERIMENTAL

### 4.1. Materials and Chemicals

The materials that were used for the construction of the PECs are P3OT, PCBM as photoactive materials, amorphous poly(ethylene oxide), POMOE, with a repeating unit of  $\text{CH}_2\text{O}(\text{CH}_2\text{CH}_2\text{O})_9$  and a redox couple iodine/triiodide. ITO-glass coated with oxidized poly(3,4-ethylenedioxythiophene), PEDOT counter electrode. Solvents such as deionized water, acetone, isopropyl alcohol and ethanol were also used for washing purpose. The chemical structures of the conjugated polymers and the acceptor molecule used in this work are depicted in Fig. 4.1.

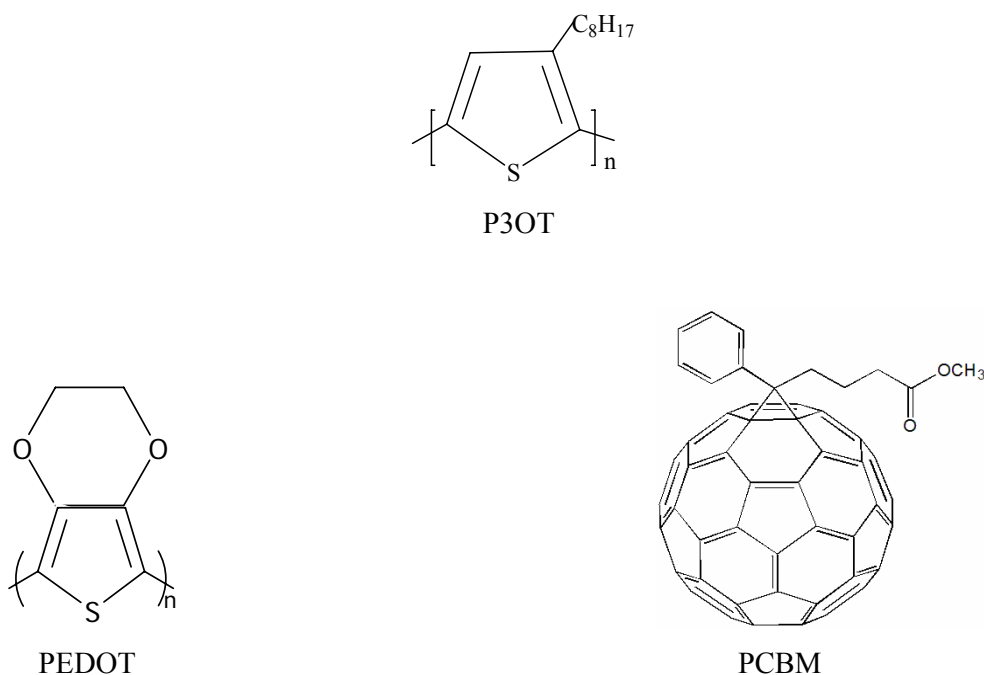


Fig. 4.1. The chemical structure of conjugated polymers used in this work and the acceptor molecule, phenyl-C<sub>61</sub>-butyric acid methyl ester, PCBM.

### 4.2. Experimental Set-up

A schematic of the experimental set-up used to measure the photoelectrochemical properties of the device is shown in Fig. 4.2. It contains a power supply, lamp housing, a monochromator, a sample holder and an output-measuring instrument. A 250 W tungsten-halogen lamp regulated by an Oriel power supply (Model 66182) is used to illuminate the PEC. An electrochemical analyzer (Model CHI630A) controlled from a computer was used to measure and record the current-voltage response both in the dark and under light illumination. The photocurrent and the photovoltage produced by turning illumination manually off and on were also recorded. A grating monochromator (Model 77250) is used to select a wavelength between 300 and 800 nm introduced into the light path and scanned manually. All spectra were corrected for the spectral response of the lamp and the monochromator by normalization to the response of a calibrated silicon photodiode (Hamamatsu, model S-1336-8BK).

The white light intensity was measured with Gigahertz optik optometer with RW-37; single channel radiometric and photometric detector heads (model X 1-1). A series of neutral density filters were placed between the light source and the sample holder to vary the light intensity incident on the sample.

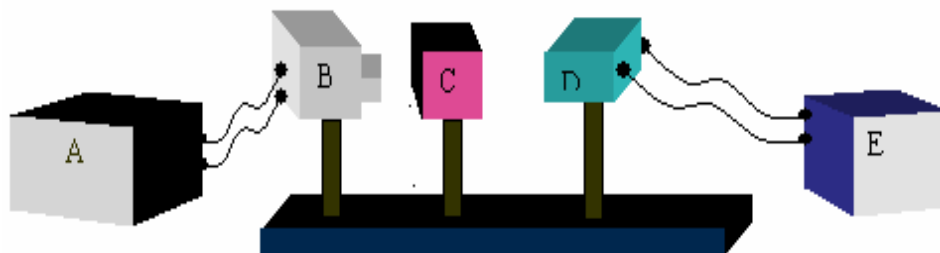


Fig. 4.2. General experimental set-up for the photoelectrochemical measurements.  
(A) power supply (B) lamp housing (C) monochromator (D) sample holder  
(E) an output measuring apparatus.

### 4.3. Procedure

#### **4.3.1. ITO-Coated Glass Preparation**

The ITO coated glass is cut to a 2.5 cm x 1.5 cm and cleaned successively with deionized water, acetone, iso-propanol and ethanol and dried with an air gun.

#### **4.3.2. Solution preparation**

The photoactive layer was prepared by dissolving 2.5 mg P3OT in 1 ml of chloroform. A mixture of 2.5 mg P3OT and 2.5 mg PCBM was also dissolved in 1 ml chloroform solution to prepare a bulk heterojunction PEC. Photoactive electrodes were formed by drop casting solutions of P3OT: PCBM or P3OT on pre-cleaned ITO coated glass substrates.

The following solutions were prepared: 0.1 M solution of EDOT in 0.1 M LiClO<sub>4</sub>-acetonitrill and 311 mg POMOE, 48.47 mg KI, 7.41 mg I<sub>2</sub> in methanol solution. The concentration of I<sub>2</sub> was 1/10 mole ratio to that of KI. The ion concentration, as given by the ratio of oxygen atoms in the POMOE to the K<sup>+</sup> ion, taking into account both oxymethylene and oxyethylene oxygen atoms was 25. Equal volumes of these three solutions were mixed to produce the polymer and I<sub>3</sub><sup>-</sup>/I<sup>-</sup> complex solid electrolyte.

#### **4.3.3. Quasi Reference Electrode Preparation**

Silver and platinum electrodes were first cleaned. The platinum was cleaned by heating in a flame of bunsen burner and using chromic acid. Quasi Ag/AgCl reference electrode was then prepared by applying a potential of 4.6 V from a dc power source between a silver and platinum wires that were immersed in a saturated potassium chloride solution.

#### **4.3.4. Electropolymerization of EDOT**

The polymer PEDOT film was prepared by the electrochemical oxidation of the monomer EDOT in a three-electrode one-compartment electrochemical cell with ITO-coated glass working electrode, platinum foil counter electrode and quasi Ag/AgCl reference electrode. The solution used for the polymerization contained 0.1 M EDOT in 0.1 M LiClO<sub>4</sub>-acetonitrile. The polymerization was carried potentiostatically at 2 V for three seconds; the

ITO-coated glass surface was covered with light blue PEDOT. The oxidized form of the polymer was rinsed with acetonitrile and dried in air.

#### 4.3.5. Preparation of the polymer P3OT and P3OT: PCBM films on ITO

The photoactive electrodes were formed by drop casting solutions of P3OT or P3OT:PCBM blend on pre-cleaned ITO coated glass substrates. After the film was dried POMOE complexed with an  $I_3^-/I^-$  redox couple was drop casted on top and was left for drying.

#### 4.3.6. Devices structure

The PEC was constructed by pressing together the photoactive electrode covered with electrolyte film and the PEDOT coated on ITO counter electrode. Then, the devices were mounted in a sample holder with  $1\text{ cm}^2$  opening to allow light from the source.

The general device structure of the solid-state PECs used in this study is shown in Fig. 4.3. It contains electrically conducting conjugated polymer, an ionically conducting polymer electrolyte, POMOE complexed with iodide/triiodide redox couple, and a counter electrode PEDOT coated on ITO. Illumination of the device was done through the ITO/photoactive layer (back side) or the PEDOT/ITO (front side).

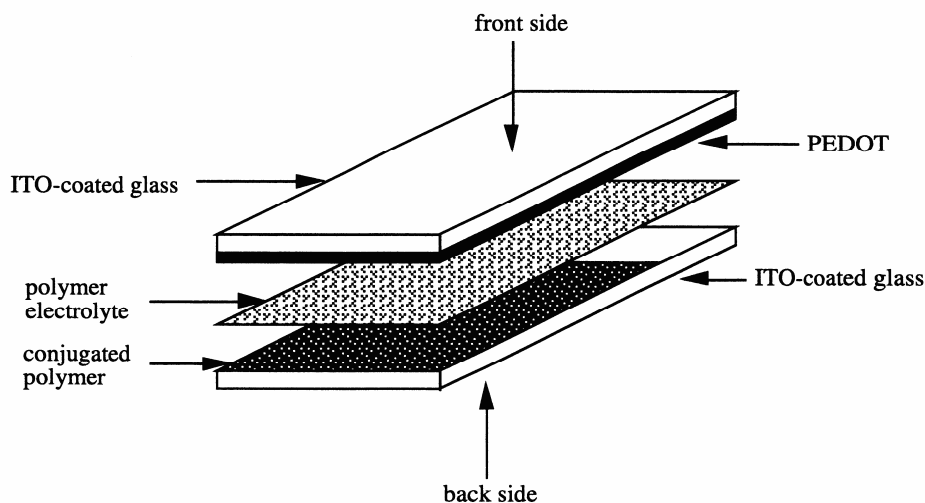


Fig. 4.3. The basic structure of the solid-state PECs.

## 5. RESULTS AND DISCUSSION

## 5.1. Current-voltage Characteristics

The current density-voltage characteristics of ITO | P3OT | POMOE:I<sub>3</sub><sup>-</sup>/I<sup>-</sup> | PEDOT | ITO and ITO | P3OT:PCBM | POMOE:I<sub>3</sub><sup>-</sup>/I<sup>-</sup> | PEDOT | ITO based solid-state PECs in the dark and under illumination with the light intensity of 100 mW cm<sup>-2</sup> from the front side illumination, are shown in Fig. 5.1 and 5.2 respectively.

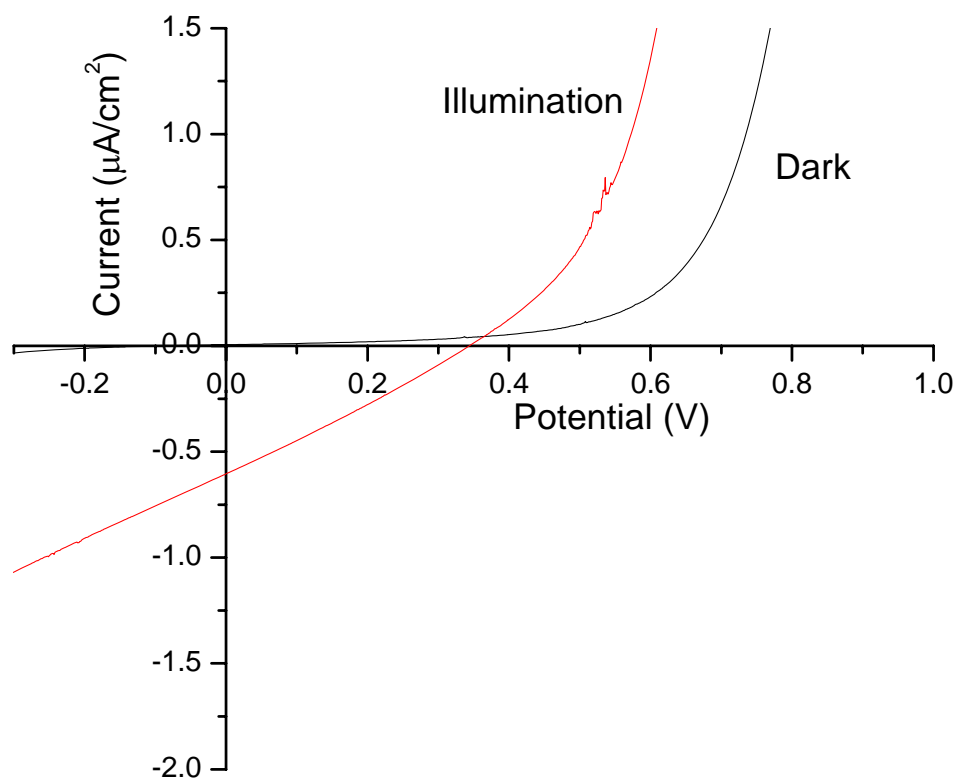


Fig. 5.1. Current-voltage characteristics of ITO | P3OT | POMOE:I<sub>3</sub><sup>-</sup>/I<sup>-</sup> | PEDOT | ITO in the dark and light from the front side illumination with light intensity of 100 mWcm<sup>-2</sup>.

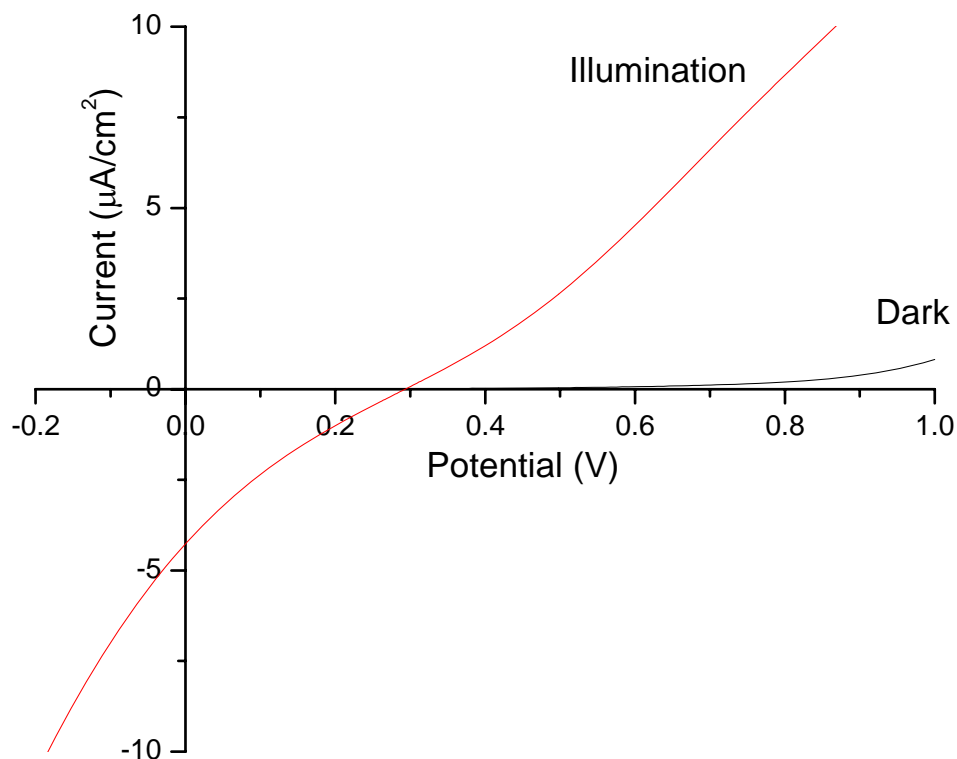


Fig. 5.2. Current-voltage characteristics of ITO | P3OT:PCBM | POMOE:I<sub>3</sub><sup>-</sup>/I<sup>-</sup> | PEDOT | ITO PECs in the dark and under illumination through front side with light intensity of 100 mWcm<sup>-2</sup>.

The devices exhibited a diode behavior in the dark, which indicates that the cells have desirable photoelectrochemical property. During illumination, cathodic photocurrents were observed at cathodic potentials, which is also indicate that the neutral conducting polymer P3OT behaves as a p-type semiconductor. This result is also confirmed by the anodic shift in the open-circuit voltage obtained under illumination. The cathodic photocurrent is due to photoinduced minority carrier (electron) injection from the P3OT electrode to the solid polymer electrolyte, where they react with the electron acceptor triiodide to produce iodide. The electrolyte contains no photoactive species; therefore, the solar energy conversion is due to solely photoexcitation of the P3OT. The holes generated during illumination go to the back (ITO/P3OT).

Similar behaviour was noticed for P3OT:PCBM based PEC. However, the results show that P3OT: PCBM composite photoactive electrode PEC has larger  $I_{sc}$  and smaller  $V_{oc}$  as compared to that of pure P3OT. The photogenerated electrons transfer from *p*-type conjugated polymer to PCBM, since the LUMO of the acceptor PCBM is lower than that of the donor P3OT, the photoexcited electrons would relax into the PCBM LUMO and separate from the holes. This electron transfer is known to take place  $\sim 1000$  times faster than any decay of the photoexcitation [37]. Thus, the increase of  $I_{sc}$  is related to the better charge transfer in P3OT:PCBM composite electrode. This phenomenon decreased recombination of electrons with holes and hence increased the photocurrent of the PEC based on the blend of P3OT and PCBM. The reason for the decrease in  $V_{oc}$  is not yet clear. However, it is assumed that in two component charge transfer systems deviations of the  $V_{oc}$  from the results of pure electronically conducting polymer devices may be due to some part of the available difference in electrochemical energy is used internally by the charge transfer to a lower energetic position on the electron acceptor [38].

The I-V curve helps us to determine the  $I_{sc}$ ,  $V_{oc}$  and the rectifying properties of the devices and also enables to calculate the fill factor. The fill factor (FF) is a measure of the maximum power obtainable from a solar cell with reference to a hypothetical maximum power, i.e., the product,  $I_{sc} V_{oc}$ . The fill factor for P3OT: PCBM based devices is lower than that of P3OT based devices, due to space-charge effects inherent in bulk heterojunction structures. The photoelectrochemical parameters obtained from the I-V characteristics of P3OT:PCBM composite based solid-state PEC as compared to that of the pure P3OT are shown in Table 2.

Table 2. Photoelectrochemical properties for the solid state PECs under the same illumination condition.

<b>Photoactive electrode</b>	<b><math>V_{oc}</math> (mV)</b>	<b><math>I_{sc}</math> (<math>\mu\text{A cm}^{-2}</math>)</b>	<b>FF</b>
P3OT	344	0.604	0.271
P3OT:PCBM	294	4.271	0.197

## 5.2. Transient Studies

The time dependence of short-circuit current density and open circuit voltage were studied for both the polymer and polymer-PCBM mixture from the front side illumination. The short-circuit current density induced by the periodical blocking of the light path to the samples are shown in Fig. 5.3 and Fig. 5.4 for ITO | P3OT | POMOE:I<sub>3</sub>/I | PEDOT | ITO and ITO | P3OT:PCBM | POMOE:I<sub>3</sub>/I | PEDOT | ITO based devices, respectively.

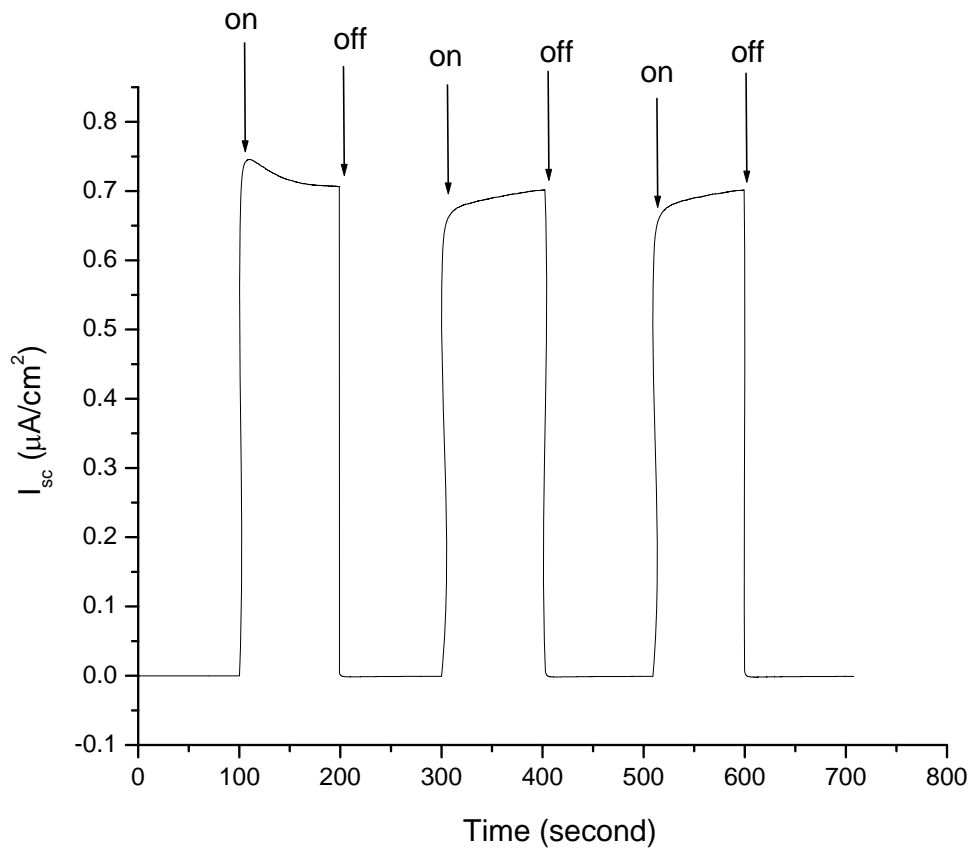


Fig. 5.3. Photocurrent response to switching illumination on and off from the front side of the P3OT based solid-state PEC with a light intensity of  $100 \text{ mW}/\text{cm}^2$ .

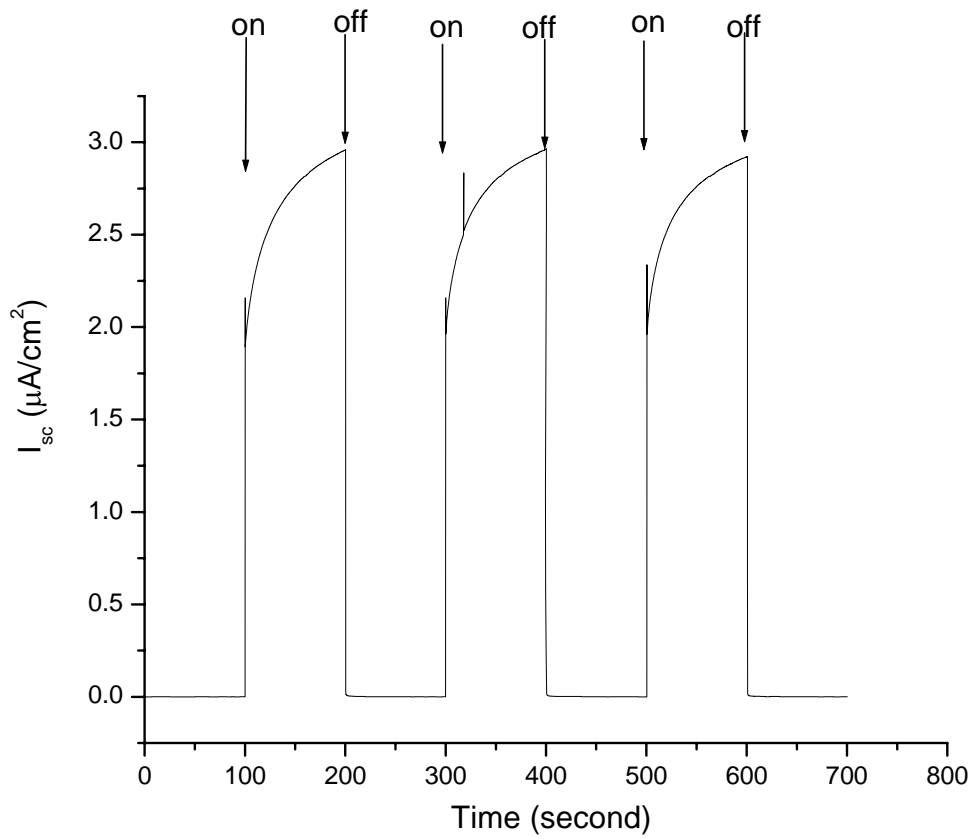


Fig. 5.4. Photocurrent response to switching illumination on and off from the front side of the P3OT:PCBM based solid-state PEC with a light intensity of  $100 \text{ mW}/\text{cm}^2$ .

Illumination of the PEC cells with white light resulted in an immediate increase in the cathodic photocurrent, which remains constant until the light is blocked. The steady state  $I_{sc}$  for the PEC based on P3OT was  $0.716 \mu\text{A cm}^{-2}$  while for that based on a blend of P3OT and PCBM was  $2.95 \mu\text{A cm}^{-2}$ . When the light was blocked, the current decayed to zero value immediately. The value of the  $I_{sc}$  is found to be larger for P3OT/PCBM than P3OT based device. This indicates that the photocurrent can be improved in the presence of PCBM acceptor.

The  $V_{oc}$  induced by the periodical blocking of the light path to the sample from the front side P3OT and P3OT:PCBM are shown Fig. 5.5 and Fig. 5.6, respectively.

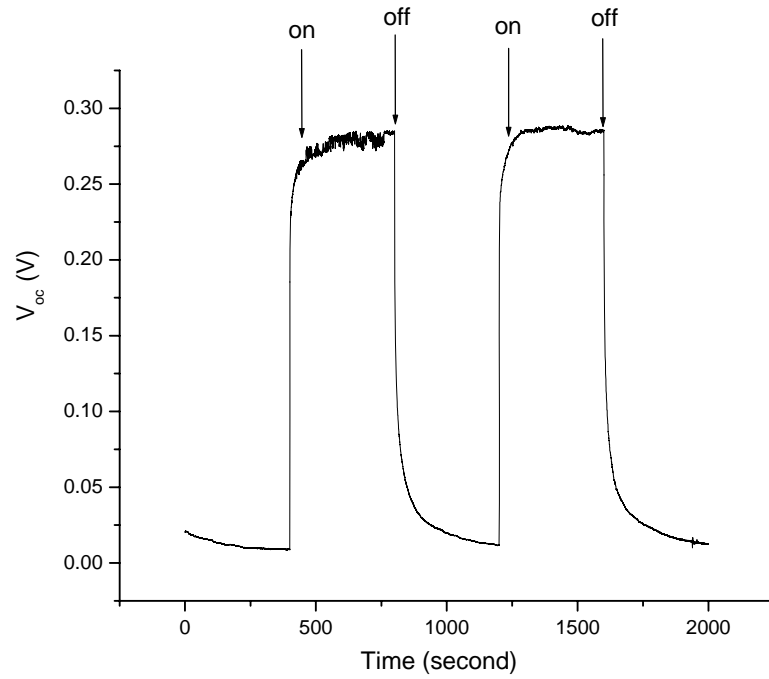


Fig. 5.5.  $V_{oc}$  response to switching illumination on and off from the front side of the P3OT based solid-state PEC with a light intensity of  $100 \text{ mW/cm}^2$ .

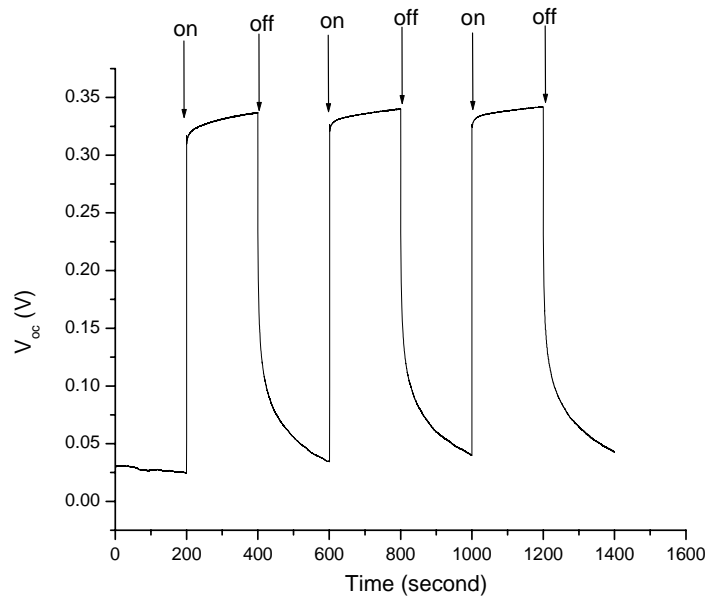


Fig. 5.6.  $V_{oc}$  response to switching illumination on and off from the front side of the P3OT:PCBM based solid-state PEC with a light intensity of  $100 \text{ mW/cm}^2$ .

The open-circuit voltage increased immediately when the P3OT based PEC was illuminated from the front side reaching a steady state value of 0.285 V and decreased slowly to a potential of about 0.008 V when the light was switched off. Similarly illumination of PEC based on a P3OT:PCBM, the  $V_{oc}$  reached a steady state value of about 0.324 V and decreased slowly to a potential of 0.025 V, when the light was switched off.

### 5.3. Spectral Response

The photocurrent collected at different wavelength relative to the number of photons incident on the surface at that wavelength determines the spectral response of the device (sometimes known as the quantum efficiency or collection efficiency at each wavelength). Light of different wavelengths is absorbed at different depths in the conjugated polymer film. The ability of a solar cell to generate photocurrent at a given wavelength of the incident light is measured by the incident monochromatic photon to current conversion efficiency (IPCE), defined as the number of electrons generated per number of incident photons. The photoresponse action spectra of the solid polymer electrolyte PEC illuminated through the front and back sides are shown in Fig. 5.7 plotted as IPCE vs. excitation wavelength.

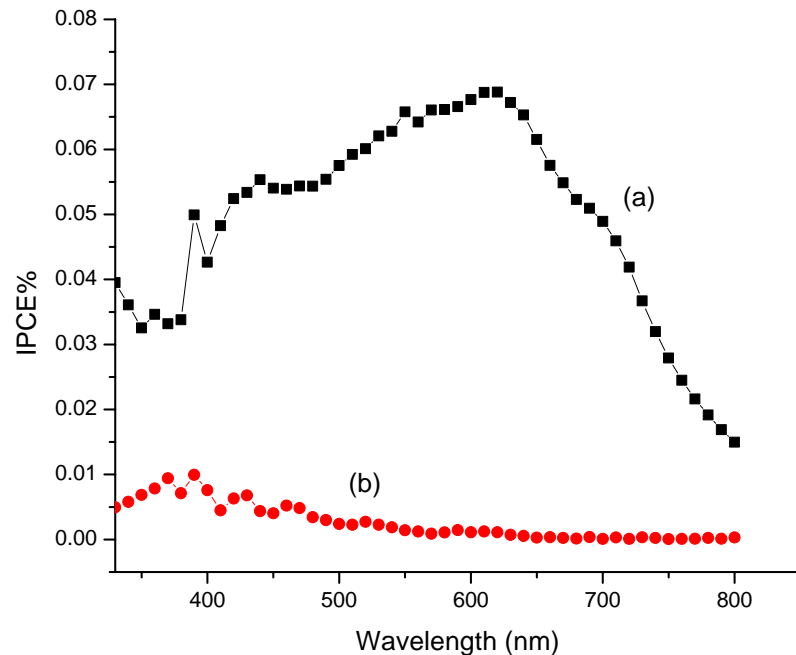


Fig. 5.7. Photocurrent action spectra through (a) front side and (b) back side of ITO | P3OT:PCBM | POMOE:I3<sup>+</sup>/I<sup>-</sup> | PEDOT | ITO PEC with monochromatic light.

The plots suggest that these solar cells can efficiently convert visible light in the region between 400 and 700 nm to photocurrent when illuminated from the front side. Comparison of front and backside conversion efficiencies showed that front side illumination has greater IPCE than backside illumination at the maximum absorbance for the cells. The highest IPCE obtained at the peak position was 0.0682 % for front side and 0.0011 % for back side illumination at 620 nm. The reason for decreasing IPCE for the back side is due to the optical filtering effect of the conjugated polymer films. When light is illuminated from the backside only a small fraction of the excitons (electron-hole pairs) produced by light absorption reach the interface to dissociate into carriers. In addition, the presence of a high density of traps in the film reduces the number of carriers for the photocurrent generation. The greater the distance from the surface, the smaller is the probability for an exciton to reach the interface and dissociate into carriers. Due to this fact the photocurrent will be less. In addition the high value of IPCE for P3OT:PCBM composite electrode based PEC is due to greater photocurrent of the cell.

#### **5.4. $I_{sc}$ dependence on incident light intensity**

The dependence of  $I_{sc}$  on incident light intensity for P3OT and P3OT:PCBM based devices are shown in Fig. 5.8 and 5.9 respectively.

These shows that the dependence of short-circuit current on the incident light intensity for the two PECs. The illumination intensity was varied from 1 to 100  $\text{mWcm}^{-2}$ . The slope ( $\alpha$  value) of  $\log I_{sc}$  vs  $\log P_{in}$  is 0.925 for pure P3OT based PEC and 0.4399 for P3OT:PCBM composite PEC. The  $\alpha$  value for the P3OT:PCBM based device is smaller than the P3OT based device. The less  $\alpha$  value of P3OT:PCBM based device can be due to more recombination site.

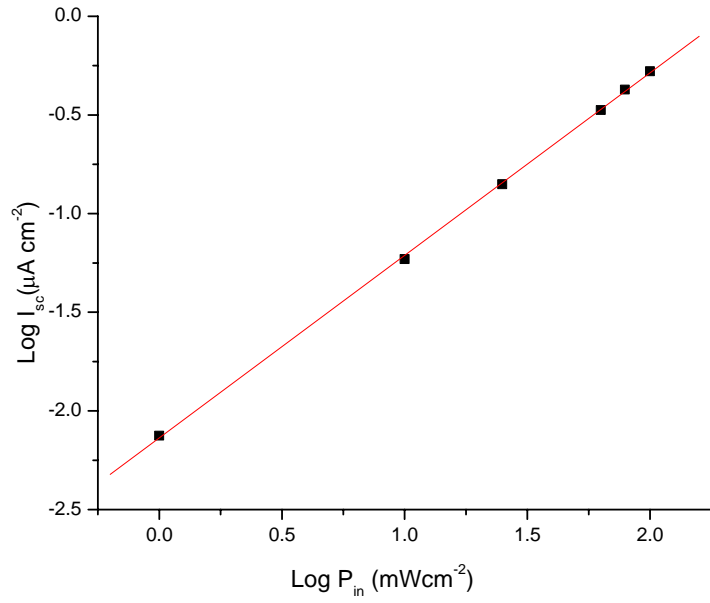


Fig. 5.8. Dependence of  $I_{sc}$  on incident light intensity of P3OT from the front side illumination

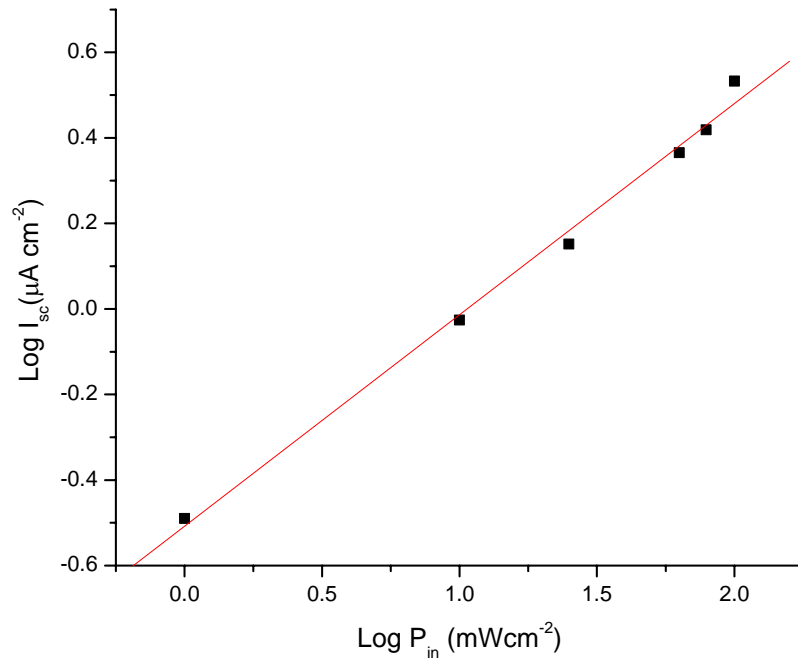


Fig. 5.9. Dependence of  $I_{sc}$  on incident light intensity of P3OT:PCBM from the front side illumination

### 5.5. $V_{oc}$ dependence on incident light intensity

As can be seen from Eq. (5),  $V_{oc}$  increases logarithmically with the light intensity because  $I_{ph}$  is linearly proportional to the incident light intensity. This is agreement with the behaviour of Schottky barrier solar cells and other organic semiconductor photoelectrode [8-14].

The dependence of on  $V_{oc}$  incident light intensity for P3OT and P3OT:PCBM based devices are shown in Fig. 5.10 and 5.11 respectively. As expected, the open circuit voltage increases rapidly at lower intensities and begins to saturate at higher intensities.

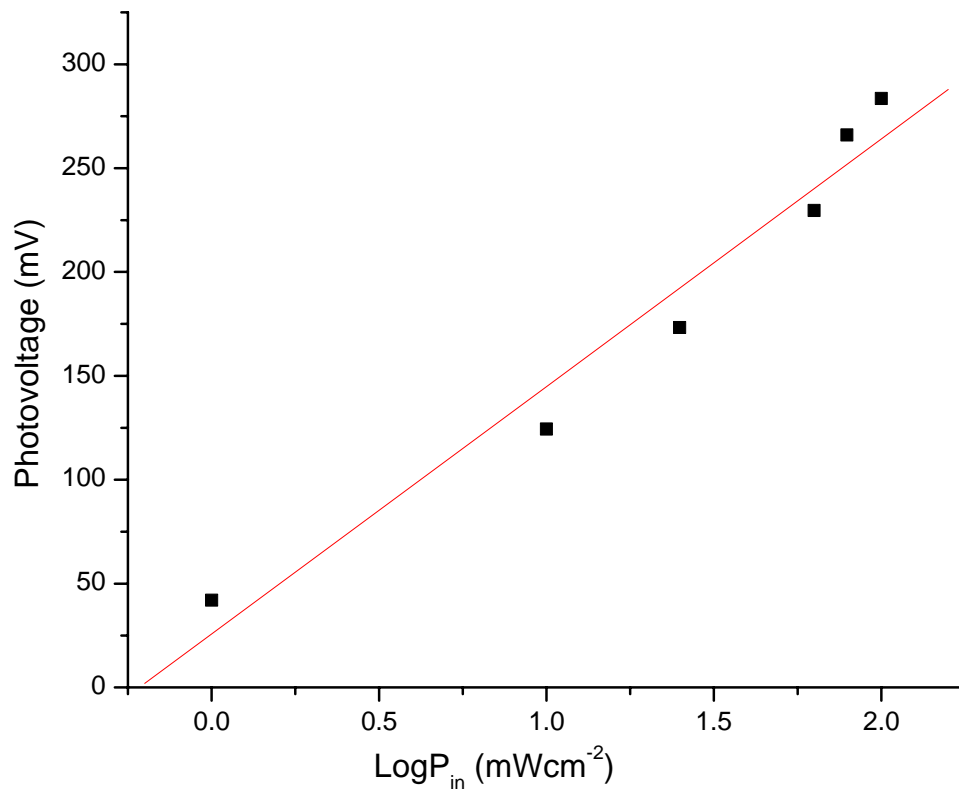


Fig. 5.10. Dependence of  $V_{oc}$  on incident light intensity of P3OT from front side illumination

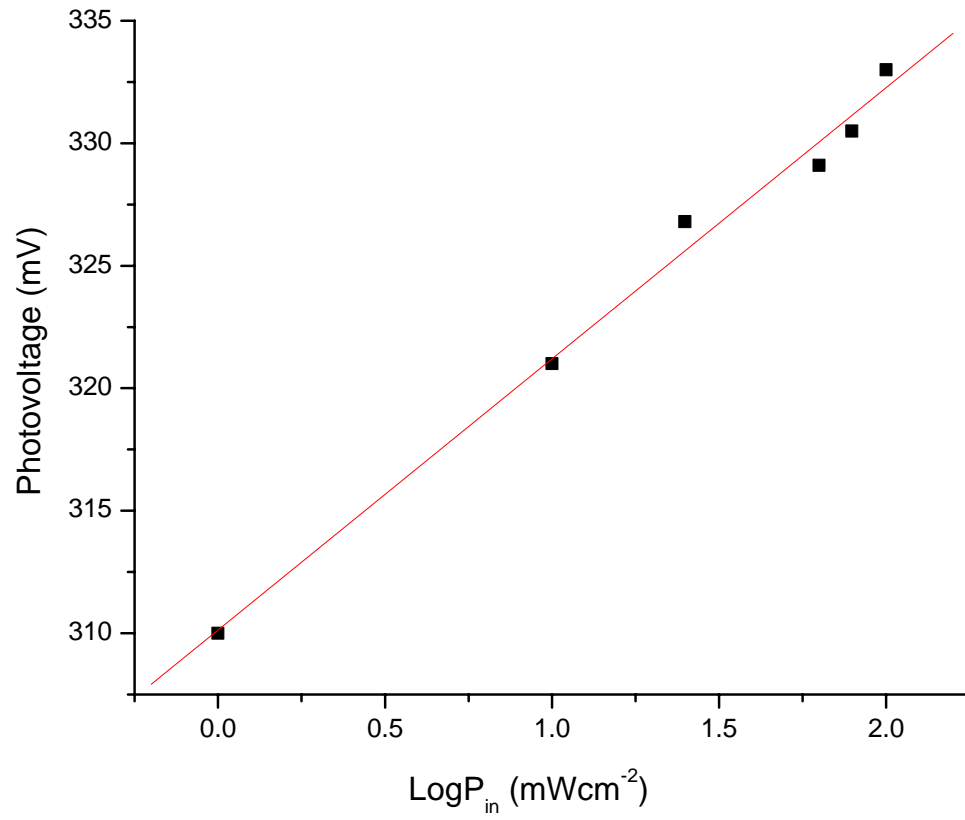


Fig. 5.11. Dependence of  $V_{oc}$  on incident light intensity of P3OT:PCBM from front side illumination

## **4. CONCLUSIONS**

A solid-state PEC based on P3OT and P3OT: PCBM photoactive electrode were constructed and studied. An open-circuit voltage of 344 mV, a short-circuit current of  $0.604 \mu\text{A cm}^{-2}$  and fill factor of 0.271 were obtained for the PEC based on P3OT as a photoactive material. While an open-circuit voltage of 294 mV, a short-circuit current of  $4.271 \mu\text{A cm}^{-2}$  and fill factor of 0.197 were obtained for the PEC based on P3OT: PCBM photoactive electrode when illuminated with the light intensity of  $100 \text{ mWcm}^{-2}$ .

The monochromatic photon to current conversion efficiency under illumination through front side and backside at maximum absorption (620 nm) were 0.0682 % and 0.011 % respectively. The  $V_{oc}$  increased sharply with increasing incident light intensity and saturated at higher intensity. The addition of PCBM on to the polymer greatly enhances the solar energy conversion performance of the polymer; due to less electrons and holes recombination rates.

## **6. REFERENCES**

1. A. Jäger-Waldau, PV Status Report 2003, European Commission, EUR 20850 EN.
2. B. A. Sandén, Materials Availability for Thin-Film PV and the Need for ‘Technodiversity’, at the EUROPV 2003 Conference 2003, Bologna (Italy).
3. C. K. Chiang, C. R. Fincher, Y. W. Park, A. J. Heeger, H. Shirakawa, E. J. Louis, S. C. Gau, A. G. MacDiarmid, *Phys. Rev. Lett.*, *39* (1977) 1098.
4. H. Shirakawa, E. J. Louis, A. G. MacDiarmid, C. K. Chiang, A. J. Heeger, *J. Chem. Com.*, *16* (1977) 578.
5. W. Ma, C. Yang, X. Gong, K. Lee, A. J. Heeger, *Adv. Funct. Mater.*, *15* (2005) 1617.
6. H. Hailin, S. ChinKung, L. MeiYang, M. E. Nicho, solar energy material and solar cells., *93* (2009) 51.
7. S. E. Shaheen, C. J. Brabec, F. Padinger, T. Fromherz, J. C. Hummelen, and N. S. Sariciftic, *Appl. Phys. Lett.*, *78* (2001) 841.
8. Teketel Yohannes and O. Inganas, *J. Electrochem. Soc.*, *143* (1996) 2310.
9. Teketel Yohannes and O. Inganas, *Solar energy and Solar Cells.*, *51* (1998) 193.
10. Teketel Yohannes, and O. Inganas, *Synth. Met.*, *107* (1999) 97.
11. M. Adi, Teketel Yohannes and T. Solomon, *Solar Energy Materials and Solar Cells.*, *83* (2004) 301.
12. T. Lemma and Teketel Yohannes, *J. Braz. Chem. Soc.*, *18* (2007) 818.
13. U. Mengesha, Teketel Yohannes, *Solar Energy Materials and Solar Cells.*, *90* (2006) 3508.
14. A. Asrat, A. Sergawie and Teketel Yohannes, *SINET: Ethiop. J. Sci.*, *30* (2007) 85.
15. J. C. Hummelen, B. W. Knight, F. LePeq, F. Wudl, J. Yao, and C. L. Wilkins. *J. Org. Chem.*, *60* (1995) 532.
16. G. Zerza, C. J. Brabec, G. Gerullo, S. De Silvestri, and N. S. Sariciftic, *Synth. Met.*, *119* (2001) 637.
17. F. W. Billmeyer, *Textbook of polymer Science*, John Wiley & Sons, Inc, New York., (1971).
18. G. Hadziioannu, P. F. van Hutten; “Semiconducting Polymers, Chemistry Physics and Engineering”; Wiley, Weinheim, (2000).
19. A. Zen, J. Pflaum, S. Hirschmann, W. Zhuang, F. Jaiser, U. Asawapirom, J. P. Rabe, U. Scherf, D. Neher, *Adv. Func. Mater.*, *14* (2004) 757.
20. A. J. Heeger, S. Kivelson, J. R. Schrieffer, W. P. Su, *Rev. Mol. Phys.*, *60* (1988) 782.

21. A. B. Kaiser, "Electronic properties of conjugated polymers", in: H. Kuzmany M. Mehring, S. Roth (ed.), Heidelberg: Springer Verlag, (1987).
22. S. Kivlson, Phys. Rev. B., 25 (1982) 3798.
23. Teketel Yohannes, Leading Edge Research in Solar Energy Rivers, Nova science publisher, Inc. New York, (2007) 105.
24. D. J. Wilson, C. V. Nicholas, R. H. Mobbs, C. Booth, J. Br. Polym., 22 (1990) 129.
25. Assefa Sergawie Solar Energy Conversion Based On Organic and Organic/Inorganic Hybrid Solar Cells, (2007), PhD thesis, Addis Ababa University, Ethiopia.
26. C. Y. Hsiang, H. Jianhui, Z. Shaoqing, L. Yongye, Y. Guanwen, Y. Yang, Y. Luping, W. Yue, L. Gang, Nature Photonics., 3 (2009) 649.
27. D. Vacar, E. S. Maniloff, D. W. McBranch, A. J. Heeger. Phys. Rev B., 56 (1997) 4573.
28. M. Kaur, A. Gopal, R. M. Davis, J. R. Hefin, solar energy material and solar cells., 93 (2009) 1779.
29. L. Smilwitz, N. S. Saricifitci, R. Wu, C. Gettinger, A. J. Heeger, F. Wudl, Phys. Rev B, (1993) 13835.
30. A. M. Ismail, T. Soga, T. Jimbo, Solar Energy Materials and Solar Cells., 94 (2010) 1406.
31. Q. Pei, G. Zuccarello, M. Ahlskog and O. Inganas, polymer., 35 (1994) 1347.
32. Teketel Yohannes, All solid state photoelectrochemical Solar Energy Conversion, (1997), PhD thesis, AAU, Ethiopia.
33. A. Heller, Acc. Chem. Res., 14 (1981) 154.
34. A. J. Nozik, Ann. Rev. Phys. Chem., 29 (1978) 189.
35. R. Memming, Elctrochem. Acta., 25 (1980) 77.
36. S. C. Jain, T. Aernout, A. K. Kapoor, V. Kumar, W. Geens, Synth. Met., 148 (2005) 245.
37. L. Smilwitz, N. S. Saricifitci, R. Wu, C. Gettinger, A. J. Heeger, F. Wudl, Phys. Rev. B., (1993) 13835.
38. C. J. Brabec, N. S. Sarcifitci, J. C. Hummellen, Adv. Funct. Mater., 11 (2001) 15.